Photo- and Thermoresponsive Polymersomes for Triggered Release**

Esther Amstad, Shin-Hyun Kim, and David A. Weitz*

Polymersomes are vesicles, the membrane of which is composed of a bilayer of amphiphilic block-co-polymers;[1] they are versatile carrier systems that can simultaneously encapsulate hydrophilic materials in their core and hydrophobic materials in their membrane.[2] By comparison to liposomes, polymersomes exhibit enhanced stability and lower permeability because of their thicker and more robust membrane.[1,2b,3] Moreover, by contrast to liposomes the chemical composition and thickness of polymersome membranes can be adjusted by tuning the length and composition of the amphiphilic block-co-polymers.[1,2b,c] This enables encapsulation of hydrophobic materials within the polymersome membrane; for example, it is possible to encapsulate nanoparticles within the membrane. By contrast, nanoparticles with diameters above 7 nm cannot be encapsulated within membranes of liposomes; this is energetically unfavorable and leads instead to micelle formation.[5] Polymersomes can be produced with precisely controlled size and structure using microfluidic technologies; moreover, these techniques enable high encapsulation efficiencies.[6] The superior stability of polymersomes, and the control of their size, structure, and encapsulation efficiency achieved with microfluidic technologies render polymersomes attractive alternatives to liposomes as delivery vehicles of active materials. However, many practical applications of polymersomes also require triggered release of encapsulants. Considerable effort has been devoted to the design of delivery vehicles that respond to changes of pH, temperature, salts, or the presence of enzymes;[2b,c] however, such stimuli can damage delicate biological system. One strategy to trigger release without

modifying conditions of the entire system is to incorporate magnetic or metallic nanoparticles into the vesicle membrane.[7] For example, vesicles containing superparamagnetic nanoparticles in their membranes can release encapsulants upon application of an alternating magnetic field because of localized heating of the magnetic nanoparticles.[8] An alternative, more practical, and facile stimulus is light, which can induce localized heating and subsequent release of encapsulants because of photothermal effects; however, this requires the use of metallic nanoparticles embedded within thermoresponsive membranes.[9] The typical method to produce such vesicles is bulk hydration; however, this results in low encapsulation efficiency and highly polydisperse polymersomes. Thus, a microfluidic approach to produce monodisperse photoresponsive polymersomes that have a high encapsulation efficiency remains an important challenge.

Herein, we report a microfluidic approach to produce thermo- and photoresponsive polymersomes with controlled size and high encapsulation efficiency. Using a capillary microfluidic device, we prepare water–oil–water (W/O/W) double-emulsion drops as templates: The middle oil phase contains a mixture of thermoinsensitive amphiphiles, thermosensitive amphiphiles, and photothermal gold nanoparticles. The resulting polymersomes consist of bilayers of amphiphiles, both thermosensitive and inert, and contain the nanoparticles within the hydrophobic portion of the shell. The polymersomes release their encapsulants if the temperature is increased above the lower critical solution temperature (LCST) of the thermoresponsive amphiphiles; they also release encapsulants upon laser illumination which causes heating through the nanoparticles. We demonstrate selective rupture of thermo- or photoresponsive polymersomes from mixtures containing responsive and nonresponsive polymersomes. These responsive polymersomes fulfill the requirements of high encapsulation efficiency, good monodispersity, low passive permeability, and facile triggered release.

We use capillary microfluidic devices to produce monodisperse W/O/W double-emulsion drops as templates to form polymersomes.[6a] The device consists of two tapered cylindrical capillaries inserted in one square capillary as shown in Figure 1a; the left cylindrical capillary is treated to be hydrophobic and used to inject the innermost aqueous phase, whereas the right capillary is treated to be hydrophilic and used to collect the double-emulsion drops. As the innermost phase, we inject an aqueous solution of 10 wt% of poly(ethylene glycol) (PEG) through the injection capillary; this solution also contains model encapsulants which are a green dye, 8-hydroxyl-1,3,6-pyrenetrisulfonic acid trisodium salt, and a red dye, sulforhodamine B. The middle oil phase is a mixture of chloroform and hexane, with a volume ratio of 40:60, containing 5 mg mL^{-1} PEG-b-poly(lactic acid) (PLA) diblock copolymers; to render the membranes thermores-

[*] Dr. E. Amstad,[+] Prof. Dr. S.-H. Kim,[+] Prof. Dr. D. A. Weitz
 School of Engineering and Applied Sciences
 Department of Physics, Harvard University
 Cambridge, MA 02138 (USA)
 E-mail: weitz@seas.harvard.edu
 Homepage: http://weitzlab.seas.harvard.edu/
 Prof. Dr. S.-H. Kim[+]
 Department of Chemical and Biomolecular Engineering
 KAIST, Daejeon (South Korea)

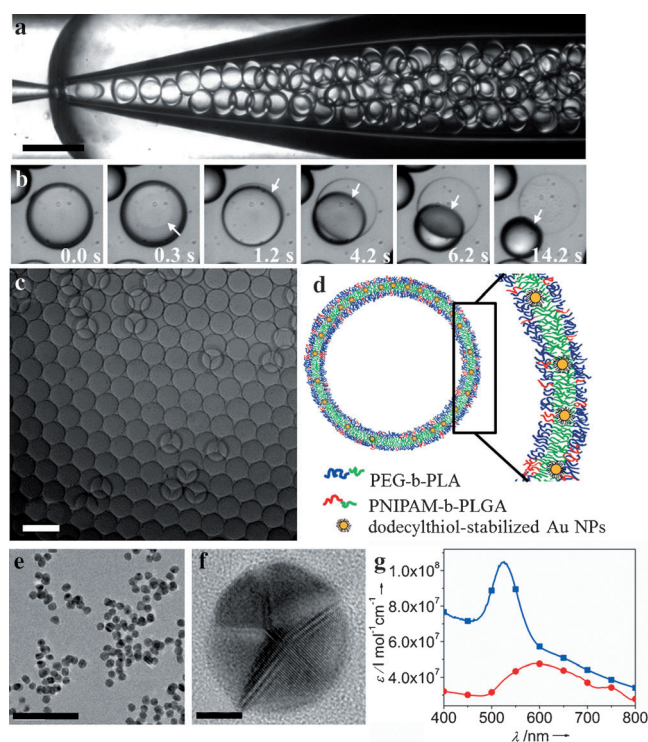 [+] These authors contributed equally to this work.

Figure 1. a) Optical microscope image showing the generation of double-emulsion drops in a capillary microfluidic device (scale bar = 500 μm). b) A series of optical microscope images showing dewetting of the middle phase on the surface of the innermost drop, leading to the formation of polymersomes; each image is taken at the time denoted on the image after the onset of dewetting, and in each image a dewetting edge is indicated with an arrow. c) Optical microscope image of monodisperse polymersomes (scale bar = 200 μm). d) Schematic illustration of the polymersomes, the membrane of which is composed of a bilayer of PEG-b-PLA and PNIPAM-b-PLGA diblock copolymers, where dodecylthiol-stabilized gold nanoparticles are doped into the hydrophobic part of the bilayer. e) Transmission electron microscope (TEM; scale bar = 100 μm) and f) high-resolution TEM images of gold nanoparticles (scale bar = 5 nm). g) The molar absorption coefficient ε of gold nanoparticles dispersed in water (blue ■) and dodecylthiol-stabilized gold nanoparticles dispersed in chloroform (red ●) is shown.

ponsive we add poly(N-isopropylacrylamide) (PNIPAM)-b-poly(lactic-co-glycolic acid) (PLGA) diblock copolymers and to render the membrane photoresponsive, we add dodecylthiol-stabilized gold nanoparticles with a diameter of (9 ± 2) nm into the oil phase. To form the middle phase, we inject this oil phase through the interstices of the square capillary surrounding the inner cylindrical capillary. We inject the continuous phase, a 10 wt% aqueous solution of poly(vinyl alcohol) (PVA), through the interstices of the square capillary surrounding the cylindrical collection capillary. The resulting double-emulsion drops flow through the collection capillary as shown in Figure 1a and the Movie S1 in the Supporting Information; they are collected in an aqueous solution containing 50 mM of NaCl. As chloroform in the middle phase quickly diffuses into the continuous aqueous phase, the middle phase dewets within one minute after double-emul-

sion drops are formed as shown in Figure 1b; this results in monodisperse polymersomes as shown in Figure 1c.[10]

The resulting polymersome membrane consists of PEG-b-PLA and PNIPAM-b-PLGA diblock copolymers; gold nanoparticles are located in the hydrophobic part of the bilayer. Its structure is shown schematically in Figure 1d. The encapsulated gold nanoparticles exhibit an absorption peak at 530 nm when dispersed in water as shown in Figure 1e–g. When the gold nanoparticles are dispersed in chloroform, their absorption peak is red-shifted and broadened as shown in Figure 1g. The absorption spectrum of the gold nanoparticles embedded in the hydrophobic part of the polymersomes is expected to be closer to that in chloroform than that in water because of the similar refractive indices of the PLA and PLGA (n is about 1.448) and chloroform (n is 1.4459).

To measure the thermo-response of these polymersomes as a function of the membrane composition, we prepare three different sets of polymersomes, the bilayers of which are composed of PEG-b-PLA diblock copolymers supplemented with PNIPAM-b-PLGA block-copolymers at 2, 5, and 10 wt%. To test the temperature dependence of the permeability of these polymersomes, we encapsulate a red dye in their cores. The oil of the middle phase is evaporated by incubating the polymersomes at room temperature in an open vial for one day. Thereafter, we incubate the polymersomes at 40°C, a temperature significantly above the lower critical solution temperature (LCST) of PNIPAM-b-PLGA which is 28°C. The LCST of PNIPAM-b-PLGA, measured with differential scanning calorimetry (DSC), is influenced by the presence of salt which lowers the LCST of PNIPAM.[10] The LCST of PNIPAM is further decreased by the PLGA block as hydrophobic blocks attached to the PNIPAM also lower their LCST.[11]

The fraction of polymersomes that releases the red dye is analyzed as a function of the incubation time. While polymersomes containing 2 wt% PNIPAM-b-PLGA retain the dye during the entire incubation time of 40 minutes, polymersomes containing 5 wt% PNIPAM-b-PLGA gradually release the dye because of an increased permeability of the membrane; however, the membrane retains its integrity as shown in Figure 2. If the concentration of PNIPAM-b-PLGA in the polymersome membrane is further increased to 10 wt%, the thermoresponsive polymersomes rupture resulting in a fast release of the dye. Based on these results, PEG-b-PLA polymersomes have to be supplemented with at least 5 wt% PNIPAM-b-PLGA to induce temperature sensitivity to them.

We attribute the difference in the release behavior of polymersomes containing 5 and 10 wt% PNIPAM-b-PLGA to the distribution of PNIPAM-b-PLGA in the polymersome membrane. Thermosensitive PNIPAM blocks collapse upon increasing the temperature above their LCST; this introduces defects into the polymersome membrane as the collapsed PNIPAM blocks are in direct contact with the surrounding water. If PNIPAM-b-PLGA is homogeneously distributed in the polymersome membrane, defects result in the formation of nanopores which increase the permeability of the polymersome membrane even though the polymersomes retain their integrity; we observe this release behavior for polymersomes
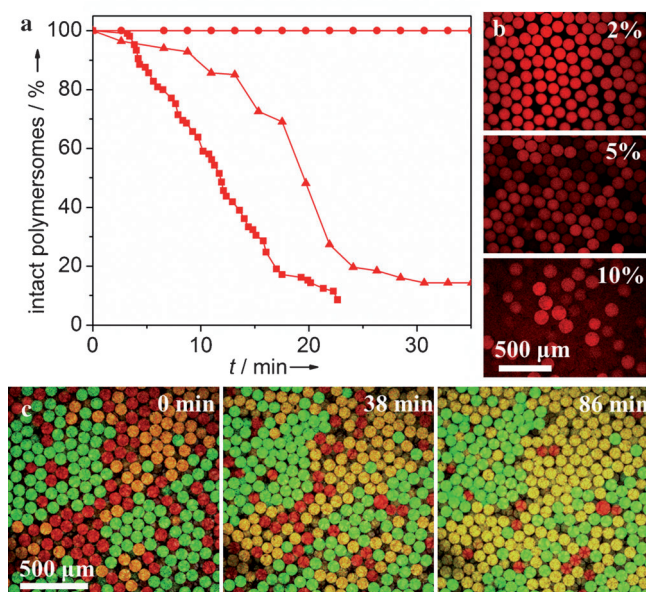
Figure 2. a) The fraction of intact polymersomes as a function of the incubation time at 40°C; three different polymersomes with membranes consisting of PEG-b-PLA and 2 wt% (●), 5 wt% (▲), and 10 wt% (■) PNIPAM-b-PLGA diblock copolymers, respectively. b) Confocal microscope images of polymersomes incubated at 40°C for 20 minutes; the concentration of PNIPAM-b-PLGA with respect to the PEG-b-PLA concentration in the polymersome membrane is 2, 5, and 10 wt% from the top. c) A series of confocal microscope images of a mixture of three different polymersomes incubated at 40°C; polymersomes composed of a bilayer of only PEG-b-PLA contain a green dye, polymersomes composed of a bilayer of PEG-b-PLA and 5 wt% PNIPAM-b-PLGA contain a red dye, and polymersomes composed of a gold nanoparticle-doped bilayer of PEG-b-PLA contain both green and red dyes and thus appear yellow. Each image is taken at the time denoted on the image.

containing 5 wt% PNIPAM-b-PLGA. By contrast, if the PNIPAM-b-PLGA and PEG-b-PLA phase separate, PNIPAM-b-PLGA microdomains are formed. A collapse of PNIPAM at temperatures above their LCST results in defects; the size of these defects is comparable to that of the PNIPAM-b-PLGA microdomains. If the size of a defect exceeds a critical value, polymersomes can no longer spontaneously heal the defects, leading to rupture of the polymersomes;[12] we observe this behavior for polymersomes containing 10 wt% PNIPAM-b-PLGA in their membrane. This suggests that the PEG-b-PLA and PNIPAM-b-PLGA phases separate to form PINPAM-b-PLGA microdomains only if the PNIPAM-b-PLGA concentration exceeds 5 wt%.

To demonstrate selective rupture of the thermoresponsive polymersomes, we incubate a mixture of thermoresponsive polymersomes consisting of PEG-b-PLA and 5 wt% PNIPAM-b-PLGA diblock polymers and inert PEG-b-PLA polymersomes with and without gold nanoparticles in their membrane at 40°C. To distinguish these three different sets of polymersomes, we encapsulate different dyes in their cores; the thermoresponsive polymersomes contain a red dye, the polymersomes consisting of only PEG-b-PLA contain a green dye, and the polymersomes consisting of PEG-b-PLA and gold nanoparticles contain a mixture of red and green dyes,

thereby appearing yellow in confocal micrographs. Upon incubation of the mixture of three different sets of polymersomes at 40°C, the thermoresponsive polymersomes release the red dye, whereas the other two types of polymersomes do not release their dyes, as shown in Figure 2c and the Movie S2 of the Supporting Information. Based on these results, we conclude that the gold nanoparticles do not significantly deteriorate the polymersome membrane as no difference in the permeability of gold nanoparticle-doped and unmodified PEG-b-PLA membranes is detected.

To create photoresponsive polymersomes, we produce polymersomes consisting of PEG-b-PLA, 5 wt% PNIPAM-b-PLGA, and gold nanoparticles; to monitor their behavior, we encapsulate a green dye in their core. As a negative control, we assemble thermoresponsive polymersomes consisting of PEG-b-PLA and 5 wt% PNIPAM-b-PLGA; to monitor their behavior, we encapsulate a red dye in their core, as shown schematically in Figure 3a. We use confocal microscopy to investigate the photoresponse of the mixture of polymersomes; we simultaneously irradiate the mixture with three different lasers that have wavelengths of 488, 532, and 633 nm, respectively, we employ three lasers because of the broad absorption spectrum of gold nanoparticles which is shown in Figure 1g. All polymersomes containing gold nanoparticles in their membrane rupture and release the green dye within
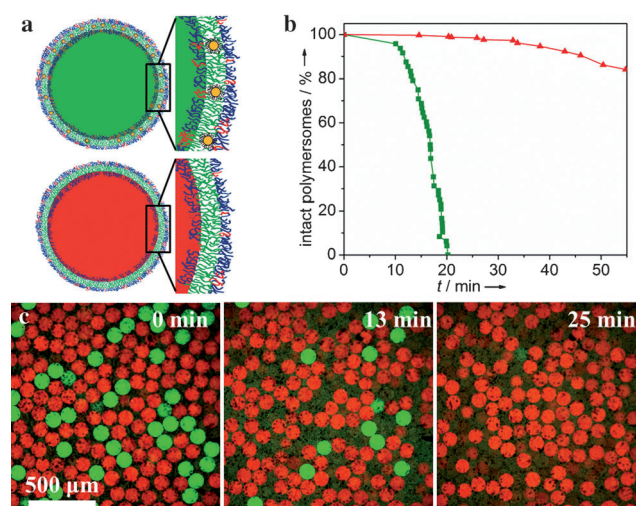

Figure 3. a) Schematic illustrations of two different polymersomes: a polymersome, the membrane of which is composed of a gold nanoparticle-doped bilayer of PEG-b-PLA and PNIPAM-b-PLGA diblock copolymers (top) and a polymersome, the membrane of which is composed of a gold-nanoparticle-free bilayer of PEG-b-PLA and PNIPAM-b-PLGA diblock copolymers (bottom). b) The fraction of intact polymersomes during laser irradiation at room temperature is shown; squares (■) correspond to polymersomes with gold nanoparticles as shown in the top image of (a) and triangles (▲) correspond to polymersomes without gold nanoparticles as shown in the bottom image of (a). c) A series of confocal microscope images of a mixture of two different types of polymersomes irradiated with the lasers at room temperature; polymersomes composed of gold-nanoparticle-doped bilayers contain a green dye as shown in the top image of (a), and polymersomes composed of gold-nanoparticle-free bilayers contain a red dye as shown in the bottom image of (a). Each image is taken at the time denoted on the image.

20 minutes if irradiated with the lasers, whereas only a marginal number of polymersomes without gold nanoparticles ruptures if exposed to the lasers for 1 hour, as shown in Figure 3b and Movie S3 in the Supporting information. The selective rupture of the polymersomes containing gold nanoparticles in their membrane indicates that the heat generated by the gold particles is highly localized.

The mechanism by which encapsulated dyes are released strongly depends on the stimulus applied to trigger release from polymersomes. The thermoresponsive polymersomes exhibit slow and sustained release of the encapsulants for 30 minutes if incubated at 40°C, while maintaining their membrane integrity, as shown in the series of confocal microscope images in Figure 4a and the first part of
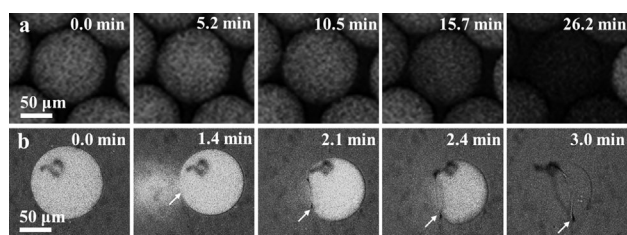

Figure 4. Series of confocal microscope images showing the different release behaviors of a) polymersomes composed of a bilayer of PEG-b-PLA and PNIPAM-b-PLGA, incubated at 40°C and b) polymersomes, composed of a gold-nanoparticle-doped bilayer of PEG-b-PLA and PNIPAM-b-PLGA, irradiated with lasers at room temperature. Each image is taken at the time denoted on the image and the arrows in (b) indicate the rupturing edge.

Movie S4 of the Supporting Information. By contrast, the photoresponsive polymersomes exhibit a sudden burst of the membrane followed by a fast release of the encapsulated dye molecules after having been irradiated with the lasers for a few minutes, as shown in Figure 4b and the second part of Movie S4. Bursting of the photoresponsive polymersomes begins with the formation of a hole in the membrane; the edge of the hole propagates through the whole polymersome. The difference in release behaviors of polymersomes induced by temperature and laser illumination reveals a clear difference in their release mechanism. An increase of the temperature above the LCST of PNIPAM results in a collective collapse of all the PNIPAM blocks present in the bilayer membrane, leading to the formation of small pores in the bilayer membranes; this allows diffusion of dye molecules, with molecular weights in the range of 100–1000 Da, through these pores, leading to a gradual release of the encapsulants without disintegration of the bilayer. By contrast, gold nanoparticles embedded in the membrane of photoresponsive polymersomes generate highly localized hot spots when irradiated. These hot spots result in a fast and localized change in the amphiphilicity of PNIPAM-b-PLGA; this leads to the formation of a hole in the membrane. The first hole that is larger than the critical size cannot heal spontaneously,[4] and this leads to complete disintegration of the bilayer.

Herein, we report a microfluidic method to fabricate monodisperse thermo- and photoresponsive polymersomes

that have a high encapsulation efficiency. Temperature sensitivity is achieved by incorporating at least 5 wt% PNIPAM-b-PLGA block copolymers into the membrane. Photosensitive polymersomes are formed by incorporating gold nanoparticles into the hydrophobic part of the membrane of thermoresponsive polymersomes. The good control over the size, as well as the narrow size distribution, high encapsulation efficiency, and the possibility to selectively trigger release of encapsulants, impart great potential to these polymersomes as delivery vehicles. In particular, the ability to trigger release of encapsulants without changing the overall solution temperature is very useful for applications that require local release of active ingredients in environments that are prone to thermal degradation. Therefore, we expect our polymersomes to be well-suited as delivery systems for many different applications that require a controlled release of encapsulants. However, before they can be used for biomedical applications, their biocompatibility must be carefully assessed to ascertain whether there is even a minute quantity of solvent remaining.

Experimental Section

Materials: We use a 10 wt% aqueous solution of PEG (weight-averaged molecular weight, M_w, 6000, Sigma–Aldrich) and a 10 wt% aqueous solution of PVA (M_w 13000–23000, Sigma–Aldrich) as innermost and continuous aqueous phases, respectively. A water-soluble green dye, 8-hydroxyl-1,3,6-pyrenetrisulfonic acid, trisodium salt (Spectrum Chemicals), and a red dye, sulforhodamine B (Aldrich) are used as model encapsulants. As a middle phase, we use a mixture of chloroform and hexane with a volume ratio of 40:60 containing 5 mgmL⁻¹ PEG (M_w 5000)-b-PLA (M_w 10000) diblock copolymers (Polyscience, Inc.). To render polymersomes thermoresponsive, we dissolve thermosensitive amphiphiles, PNIPAM-b-PLGA, into the middle phase at concentrations of 2, 5, and 10 wt% with respect to PEG-b-PLA; the PNIPAM-b-PLGA is synthesized by coupling poly(N-isopropylacrylamide) amine (M_n 5500, Sigma–Aldrich) to poly(D,L-lactide-co-glycolide) (M_w 4000–15000, Sigma–Aldrich). Photosensitivity is induced to polymersomes by adding gold nanoparticles with an average diameter of 9 nm into the middle phase at a concentration of 2 wt% with respect to PEG-b-PLA; the gold nanoparticles are produced by a seed-mediated synthesis.[12] To render nanoparticles hydrophobic, their surfaces are modified with dodecylthiol (Sigma–Aldrich). We detail the synthesis and characterization of the PNIPAM-b-PLGA and the hydrophobic gold nanoparticles in the Supporting Information.

Preparation of polymersomes: We use glass capillary microfluidic devices to produce W/O/W double-emulsion drops as templates of polymersomes; the device is composed of two tapered circular capillaries (World precision instruments, Inc., 1B100-6) inserted in one square capillary (AIT glass) as shown in Figure 1a. One cylindrical capillary is tapered to have a 80 μm diameter orifice and is treated with n-octadecyltrimethoxyl silane (Aldrich) to render it hydrophobic. The other cylindrical capillary is tapered to have a 180 μm diameter orifice and is treated with 2-[methoxy(polyethyleneoxy)propyl] trimethoxyl silane (Gelest, Inc.) to make it hydrophilic. These two cylindrical capillaries are coaxially aligned in the square capillary. Flow rates of the innermost, middle, and continuous phases are typically set to be 800, 800, and 3000 μLh⁻¹, respectively. The resultant double-emulsion drops are collected in an aqueous solution containing 50 mM NaCl; NaCl is added to match the osmotic pressure of the continuous phase with the osmotic pressure in the polymersome core. Polymersomes are incubated at room temperature

for one day without mechanical stirring to evaporate volatile oils before the polymersomes are characterized.

Analysis of triggered release: To observe the temperature response of polymersomes, we maintain the temperature of the polymersome suspension at 40°C using a microscope heating stage (Warner instruments) and observe the response of polymersomes with a confocal microscope (Leica TCS SP5). To observe the photo-response of polymersomes, we illuminate the polymersome mixture with three lasers built into the confocal microscope; they have wavelengths of 488, 532, and 633 nm, and powers of 400, 270, and 900 µW, respectively. We maintain the temperature at 25°C.

[1] B. M. Discher, Y. Y. Won, D. S. Ege, J. C. M. Lee, F. S. Bates, D. E. Discher, D. A. Hammer, *Science* **1999**, *284*, 1143–1146.

[2] a) J. S. Lee, J. Feijen, *Journal of Controlled Release* **2012**, *161*, 473–483; b) M. H. Li, P. Keller, *Soft Matter* **2009**, *5*, 927–937; c) O. Onaca, R. Enea, D. W. Hughes, W. Meier, *Macromol. Biosci.* **2009**, *9*, 129–139.

[3] D. E. Discher, A. Eisenberg, *Science* **2002**, *297*, 967–973.

[4] a) H. S. Wi, K. Lee, H. K. Pak, *J. Phys. Condens. Matter* **2008**, *20*, 494211–494217; b) M. Schulz, A. Olubummo, W. H. Binder, *Soft Matter* **2012**, *8*, 4849–4864.

[5] a) H. C. Shum, J. W. Kim, D. A. Weitz, *J. Am. Chem. Soc.* **2008**, *130*, 9543–9549; b) H. C. Shum, D. Lee, I. Yoon, T. Kodger, D. A. Weitz, *Langmuir* **2008**, *24*, 7651–7653; c) J. C. Stachowiak, D. L. Richmond, T. H. Li, A. P. Liu, S. H. Parekh, D. A. Fletcher, *Proc. Natl. Acad. Sci. USA* **2008**, *105*, 4697–4702; d) S. H. Kim, H. C. Shum, J. W. Kim, J. C. Cho, D. A. Weitz, *J. Am. Chem. Soc.* **2011**, *133*, 15165–15171.

[6] E. Amstad, E. Reimhult, *Nanomedicine* **2012**, *7*, 145–164.

[7] a) Y. J. Chen, A. Bose, G. D. Bothun, *Acs Nano* **2010**, *4*, 3215–3221; b) E. Amstad, J. Kohlbrecher, E. Müller, T. Schweizer, M. Textor, E. Reimhult, *Nano Lett.* **2011**, *11*, 1664–1670; c) K. M. Krishnan, *IEEE Trans. Magn.* **2010**, *46*, 2523–2558; d) C. Sanson, O. Diou, J. Thevenot, E. Ibarboure, A. Soum, A. Brulet, S. Miraux, E. Thiaudiere, S. Tan, A. Brisson, V. Dupuis, O. Sandre, S. Lecommandoux, *Acs Nano* **2011**, *5*, 1122–1140.

[8] a) L. Paasonen, T. Laaksonen, C. Johans, M. Yliperttula, K. Kontturi, A. Urth, *J. Controlled Release* **2007**, *122*, 86–93; b) X. Q. An, F. Zhang, Y. Y. Zhu, W. G. Shen, *Chem. Commun.* **2010**, *46*, 7202–7204; c) P. K. Jain, X. H. Huang, I. H. El-Sayed, M. A. El-Sayed, *Acc. Chem. Res.* **2008**, *41*, 1578–1586; d) J. B. Song, L. Cheng, A. P. Liu, J. Yin, M. Kuang, H. W. Duan, *J. Am. Chem. Soc.* **2011**, *133*, 10760–10763; e) M. H. Lee, K. C. Hribar, T. Brugarolas, N. P. Kamat, J. A. Burdick, D. Lee, *Adv. Funct. Mater.* **2012**, *22*, 131–138.

[9] H. C. Shum, E. Santanach-Carreras, J. W. Kim, A. Ehrlicher, J. Bibette, D. A. Weitz, *J. Am. Chem. Soc.* **2011**, *133*, 4420–4426.

[10] Y. J. Zhang, S. Furyk, D. E. Bergbreiter, P. S. Cremer, *J. Am. Chem. Soc.* **2005**, *127*, 14505–14510.

[11] H. Feil, Y. H. Bae, J. Feijen, S. W. Kim, *Macromolecules* **1993**, *26*, 2496–2500.

[12] O. Sandre, L. Moreaux, F. Brochard-Wyart, *Proc. Natl. Acad. Sci. USA* **1999**, *96*, 10591–10596.

[13] J. L. Niu, T. Zhu, Z. F. Liu, *Nanotechnology* **2007**, *18*, 325607–325614.